Published in final edited form as:
Int J Biochem Cell Biol. 2014 October ; 55: 24–34. doi:10.1016/j.biocel.2014.08.004.

Lumisterol is metabolized by CYP11A1: discovery of a new pathway

Robert C. Tuckey[a,*], **Andrzej T. Slominski**[b,c,*], **Chloe Y. S. Cheng**[a], **Jianjun Chen**[d,e], **Tae-Kang Kim**[b], **Min Xiao**[d], and **Wei Li**[d]

[a]School of Chemistry and Biochemistry, The University of Western Australia, Crawley, WA, Australia

[b]Department of Pathology and Laboratory Medicine, Center for Cancer Research, University of Tennessee Health Science Center, Memphis, TN, USA

[c]Department of Medicine, Division of Rheumatology and Connective Tissue Diseases, University of Tennessee Health Science Center, Memphis, TN, USA

[d]Department of Pharmaceutical Sciences, College of Pharmacy, University of Tennessee Health Science Center, Memphis, TN, USA

[e]Department of Pharmaceutical Sciences, School of Pharmacy, South College, Knoxville, TN, USA

Abstract

Lumisterol3 (L3) is produced by photochemical transformation of 7-dehydrocholesterol (7-DHC) during exposure to high doses of ultraviolet B radiation. It has been assumed that L3 is biologically inactive and is not metabolized in the body. However, some synthetic derivatives of L3 display biological activity. The aim of this study was to test the ability of CYP11A1 to metabolize L3. Incubation of L3 with bovine or human CYP11A1 resulted in the formation of three major and a number of minor products. The catalytic efficiency of bovine CYP11A1 for metabolism of L3 dissolved in 2-hydroxypropyl-β-cyclodextrin was approximately 20% of that reported for vitamin D3 and cholesterol. The structures of the three major products were identified as 24-hydroxy-L3, 22-hydroxy-L3 and 20,22-dihydroxy-L3 by NMR. 22-hydroxy-L3 was further metabolized by bovine CYP11A1 to 20,22-dihydroxy-L3. Both 22-hydroxy-L3 and 20,22-dihydroxy-L3 gave rise to a minor metabolite identified from authentic standard and mass spectrometry as pregnalumisterol (pL) (product of C20-C22 side chain cleavage of L3) and two trihydroxy-L3 products. The capability of tissues expressing CYP11A1 to metabolize L3 was demonstrated using pig adrenal fragments where 20,22-dihydroxy-L3, 22-hydroxy-L3, 24-hydroxy-L3 and pL were detected by LC/MS. Thus, we have established that L3 is metabolized by

Correspondence: Robert C. Tuckey, PhD, School of Chemistry and Biochemistry, The University of Western Australia, Crawley, WA 6009, Australia, Tel: 61 8 64883040, Fax: 61 8 64881148, robert.tuckey@uwa.edu.au.
*These authors contributed equally to this work.

CYP11A1 to 22- and 24-hydroxy-L3 and 20,22-dihydroxy-L3 as major products, as well as to pL and other minor products. The previously reported biological activity of pL and the presence of CYP11A1 in skin suggest that this pathway may serve to produce biologically active products from L3, emphasizing a novel role of CYP11A1 in sterol metabolism.

Keywords

CYP11A1; cytochrome P450scc; lumisterol; vitamin D3; hydroxylation

1. Introduction

Vitamin D3 is produced by the action of UVB radiation (280–320 nm spectrum of solar light) on 7-dehydrocholesterol (7-DHC) in the skin (Holick, 2003; Holick et al., 1980; MacLaughlin et al., 1982;). The initial event is the photochemical breaking of the C9-C10 bond in the B ring of 7-DHC resulting in the formation of previtamin D3 (Fig. 1). Once formed, previtamin D3 undergoes thermal isomerization in the skin over several hours to form vitamin D3. With further exposure to UVB radiation, previtamin D3 undergoes photoisomerization to lumisterol3 (L3) and tachysterol3 (T3) (Fig. 1) (Holick, 2003; Wacker and Holick, 2013). These photochemical reactions are reversible and are dependent on the temperature and UVB dose. T3 is the most photoreactive of the three isomers and sunlight drives the conversion of T3 to L3 via previtamin D3, resulting in L3 being the major photoisomer observed in human skin after prolonged UVB exposure (Holick et al., 1981; MacLaughlin et al., 1982). The conversion of previtamin D3 to L3 involves reformation of the C9-C10 bond but in a 9β,10α-configuration, making it a stereoisomer of 7-DHC.

CYP11A1, also known as cytochrome P450scc, catalyzes the first step in steroid hormone synthesis, the cleavage of the side chain of cholesterol to produce pregnenolone. This reaction involves initial hydroxylation of the cholesterol side chain in the 22*R* position, hydroxylation at C20 and then scission of the side chain between C20 and C22 (Tuckey, 2005). We and others have shown that CYP11A1 can also cleave the side chain of 7-DHC, and can hydroxylate the side chain of vitamin D3, vitamin D2 and ergosterol, producing a number of biologically active derivatives (reviewed in (Slominski et al., 2014a)). Guryev et al. (2003) and Strushkevich et al. (2011) reported that CYP11A1 hydroxylates vitamin D3 at C20 and C22 producing 20-hydroxyvitamin D3 and 20,22-dihydroxyvitamin D3 as major products. We also demonstrated the ability of CYP11A1 to hydroxylate vitamin D3 at these positions and further showed that C23 is a major site of hydroxylation with 20,23-dihydroxyvitamin D3 being the next most abundant product after 20-hydroxyvitamin D3 (Slominski et al., 2005a; Tuckey et al., 2008a, 2008b, 2011). Importantly, we have provided initial evidence that CYP11A1-initiated metabolism of 7-DHC, vitamin D3 and vitamin D2 can occur under *in vivo* conditions (Slominski et al., 2009, 2012a, 2012b, 2014a, 2014b). The novel CYP11A1-derived hydroxy-derivatives of vitamin D3 are active in inhibiting proliferation and stimulating differentiation in a range of cell types cultured *in vitro* (reviewed in (Slominski et al., 2014a)), and in reducing inflammation and skin fibrosis in mice *in vivo* (Slominski et al., 2013, 2014a), but lack the toxic and calcemic effects seen with high doses of $1,25(OH)_2D3$ (Slominski et al., 2010; Wang et al., 2012). We and others

have also reported the presence of CYP11A1 in human skin (Slominski et al., 1996, 2004, 2014a; Thiboutot et al., 2003;) and have detected CYP11A1-dependent production of 20(OH)D3 by cultured keratinocytes in the absence of exogenous vitamin D3 substrate (Slominski et al., 2012a). These findings, together with the ability of CYP11A1 to act on 7-DHC (Slominski et al., 2004, 2009, 2012b), ergosterol (Slominski et al., 2005b; Tuckey et al., 2012) and vitamin D2 (Nguyen et al., 2009; Slominski et al., 2006, 2014b) has prompted us to test the ability of this enzyme to act on L3.

2. Materials and Methods

2.1. Materials

2-Hydroxypropyl-β-cyclodextrin (cyclodextrin), vitamin D3, dioleoyl phosphatidylcholine, bovine heart cardiolipin and NADPH were from Sigma-Aldrich Pty. Ltd. (Sydney, Australia). L3 was from Toronto Research Chemicals (North York, Canada). Prior to use it was purified by HPLC on a C18 column (Grace Alltima, 25 cm × 4.6 mm, particle size 5 μm) using a 64% to 100% methanol in water gradient for 15 min followed by 100% methanol for 50 min, at a flow rate of 0.5 mL/min. Pregnalumisterol (pL) and 20-hydroxylumisterol3 (20(OH)L3) were synthesized by UVB irradiation of 7-dehydropregnenolone and 20-hydroxy-7-DHC, respectively, purified and their structure confirmed by NMR as described previously (Zmijewski et al., 2008).

2.2. Preparation of enzymes

Bovine and human CYP11A1, human adrenodoxin and human adrenodoxin reductase were expressed in *Escherichia coli* and purified as described previously (Tuckey and Sadleir, 1999; Tuckey et al., 2012, Woods et al., 1998). Highly purified bovine CYP11A1 was used for small scale metabolic and kinetic studies and was prepared from adrenal mitochondria by extraction with sodium cholate, ammonium sulfate fractionation and octyl Sepharose chromatography (Tuckey and Stevenson., 1984).

2.3. Large-scale incubations of lumisterol with bovine CYP11A1

Two 9.0 mL incubations were carried out in buffer comprising 20 mM HEPES (pH 7.4), 100 mM NaCl, 0.1 mM dithiothreitol, 0.1 mM EDTA, 2 μM expressed bovine CYP11A1, 15 μM adrenodoxin, 0.3 μM adrenodoxin reductase, 2 mM glucose 6-phosphate, 2 U/ml glucose 6-phosphate dehydrogenase and 50 μM NADPH. Stock L3 (1.8 mM) in 45% cyclodextrin (0.25 mL) was added to the incubation mixture to give a final L3 concentration of 50 μM and a cyclodextrin concentration of 1.25% (De Caprio et al., 1992; Tuckey et al., 2008b). Samples were pre-incubated for 8 min, reactions started by the addition of NADPH and incubations carried out for 3 h at 37°C with shaking. Reactions were stopped by the addition of 20 mL of ice-cold dichloromethane. After shaking and centrifugation, the lower phase was retained and the upper aqueous phase was extracted another 4 times with 20 mL dichloromethane. The combined dichloromethane extracts were dried under nitrogen at 30°C, dissolved in 2 ml methanol and filtered through a 0.1 μM syringe filter prior to purification by HPLC.

2.4. Incubations with adrenal glands

The use of pig adrenals was approved by the Animal Care and Use Committee at the UTHSC and protocols conformed to NIH guidelines. Pig adrenals were from a female Landrace cross Large White pig, 2 years old. The organs were collected using standard procedures (Slominski et al., 2014c). The incubations of adrenal fragments followed modifications of the protocols described previously (Slominski et al., 2009, 2014b). Briefly, after dissection from the adipose, the adrenals were cut with scissors into small fragments and washed with PBS. The fragments were incubated with 500 μM L3 for 20 h in tris-buffered medium (pH 7.4) containing 110 mM NaCl, 5 mM KCl, 2.5 mM $CaCl_2$, 1 mM $MgSO_4$, 1 mM KH_2PO_4, 5 mM isocitrate, 0.5 mM NADPH, 0.2% glucose, 1% BSA and 33 mM Tris-HCl. The reaction mixtures were extracted twice with 2.5 volumes of dichloromethane and extracts dried under nitrogen gas.

2.5. HPLC purification of products of lumisterol metabolism

Initial HPLC purification of L3 metabolites produced by purified CYP11A1 were carried out using a Perkin Elmer HPLC equipped with a UV monitor set at 280 nm. The filtered extract was chromatographed on a C18 column (Grace Alltima, 25 cm × 4.6 mm, particle size 5 μm) using a 64% to 100% methanol in water gradient for 15 min followed by 100% methanol for 50 min, at a flow rate of 0.5 mL/min. The five major products were collected and further purified on the same column using a 45% to 100% acetonitrile in water gradient for 25 min followed by 100% acetonitrile for 25 min, at a flow rate of 0.5 mL/min. These samples were then analyzed by mass spectrometry and/or NMR (see below), or incubated with CYP11A1 to test if they were further metabolized. The concentrations of L3 and its hydroxy-derivatives were measured using an extinction coefficient of 8,886 $M^{-1}cm^{-1}$ at 280 nm (Norval et al., 2010).

To isolate products of L3 metabolism from incubations with adrenal glands, the dried extracts were re-dissolved in methanol and subjected to RP-HPLC using a dual pump chromatography system (Waters 2695 Alliance, Milford, MA) equipped with a Waters C18 column (250 × 4.6 mm, 5 μm particle size). The separation was performed using a gradient of acetonitrile in water (40 – 100% for 15 min) at a flow rate 0.5 ml/min, followed by 100% acetonitrile for 30 min at flow rate 0.5 ml/min. Samples with RTs corresponding to standards were dried using a speed-vac drier (Savant instruments, Inc. Holbrook, NY), re-dissolved in methanol and analyzed by LC-MS as described in section 2.8.

2.6. Small-scale incubations of L3 with CYP11A1

Incubations were carried out in a similar fashion to that described above (section 2.3) for large-scale incubations except that the final cyclodextrin concentration was 0.25%, the incubation volume was typically 0.5 mL and CYP11A1 purified from bovine adrenal glands was used at concentrations ranging from 0.4 to 2 μM. For experiments to determine kinetic constants, the incubation time was 4 min. The amounts of product formed and kinetic constants were calculated as before (Tuckey et al., 2008b).

2.7. NMR spectroscopy

NMR measurements were performed using an inverse triple-resonance 3 mm probe on a Varian Unity Inova 500 MHz spectrometer (Agilent Technologies, Inc., Santa Clara, CA, U.S.A.). Sample was dissolved in CD_3OD and transferred to a 3-mm Shigemi NMR tube (Shigemi Inc., Allison Park, PA). Temperature was regulated at 22°C and was controlled with an accuracy of ± 0.1°C. Chemical shifts were referenced to residual solvent peaks for CD_3OD (3.31 ppm for proton and 49.15 ppm for carbon). Standard two-dimensional NMR experiments [^1H-^1H total correlation spectroscopy (TOCSY, mixing time=80 ms), ^1H-^{13}C heteronuclear single quantum correlation spectroscopy (HSQC), and ^1H-^{13}C heteronuclear multiple bond correlation spectroscopy (HMBC)] were acquired in order to fully elucidate the structures of the metabolites. All data were processed using ACD software (Advanced Chemistry Development, Toronto, ON, Canada), with zero-filling in the direct dimension and linear prediction in the indirect dimension.

2.8. Mass spectrometry

LC-MS of adrenal extracts partially purified by HPLC (section 2.6) was carried out using a Waters ACQUITY I-Class UPLC system (Waters, Milford, USA) connected to a Xevo™ G2-S QTof (quadrupole hybrid with orthogonal acceleration time-of-flight) tandem mass spectrometer (Waters, Milford, USA). An Agilent Zorbax Eclipse Plus C18 column (2.1 × 50 mm, 1.8 μm, Agilent Technologies, Santa Clara, CA) was used with a linear gradient of methanol in water containing 0.1% formic acid (20 – 60% for 3 min, 60 – 100% for 1 min, 100% for 2.1 min, 100 – 20% for 0.1 min) at flow rate of 0.3 mL/min. The Waters Xevo™ G2-S QTof system was also used to acquire the high resolution mass spectra on products AC, G and E utilizing an electrospray ionization (ESI) source with a Waters Acquity I-Class UPLC and BEH C18 column (2.1 mm × 50 mm, 1.7 μm, Waters, Milford, USA). Data were collected and processed by Masslynx 4.1 software.

For products F, H, I and pL, mass spectrometry was carried out by 2 dimensional UPLC tandem mass spectrometry in a similar manner to that described previously (Clarke et al., 2013). The system consisted of two Agilent 1290 UPLC binary pumps coupled to an Agilent 6460 triple quadrupole tandem mass spectrometer with a Jetstream source. The mass spectrometer was operated in the positive ESI mode.

3. Results

3.1 Analysis of metabolites of L3 produced by bovine CYP11A1

HPLC analysis revealed that incubation of L3 with bovine CYP11A1 for 90 min produced 3 major products (A, B and C) and a number of minor products (E, F and G) (Fig. 2). The only standards available for the likely products of L3 metabolism by CYP11A1 were pL which represents the product of side-chain cleavage of lumisterol between C20 and C22, and 20(OH)L3. A minor product had the same retention time as pL suggesting that some side-chain cleavage occurred (Fig. 2). No product corresponding to 20(OH)L3 standard which ran close to but distinct from product G, was observed.

A time course for L3 metabolism revealed rapid accumulation of the two major products B and C, plus the minor product G. (Fig. 2C). With longer incubation times appreciable product A was produced plus the minor products shown in Fig. 2D could be detected. These displayed appreciable lags suggesting that they are secondary products resulting from further metabolism of products A, B, C or G. The minor product with the same retention time as pL displayed a long lag, being barely detectable before 40 min (Fig. 2D), consistent with it being a secondary product. This product was collected and further analyzed by HPLC using an acetonitrile gradient (see Experimental Procedures) where it also displayed an identical retention time to pL.

To permit identification of the major products, the incubation of L3 with bovine CYP11A1 was scaled up to 18 ml and the products purified by RP-HPLC using two separate solvent systems (see Materials and Methods). This yielded 240 nmol product B, 200 nmol product C and 50 nmol Product A, each of which was subjected to high resolution mass spectrometry and NMR analysis. Minor products E and G, were collected and analyzed by high resolution mass spectrometry only. The detected positive ions of the metabolites were sodium ion adducts (Table 1) with the predicted elemental masses indicating that products B, C and G are monohydroxylumisterols while products A and E are dihydroxylumisterols.

3.2. Identification of product B as 24-hydroxylumisterol3 (24(OH)L3) by NMR

The site of hydroxylation in the monohydroxy-L3, product B, was assigned to be at the 24-position based on the NMR spectra for this metabolite. First, none of the five methyl groups (18, 19, 21, 26, 27) are hydroxylated based on ^{1}H NMR and ^{1}H-^{13}C HSQC (Fig. 3A and B). ^{1}H-^{13}C HSQC revealed the presence of a new methine group at 3.22 ppm (^{13}C at 78.4 ppm, Fig. 3C). ^{1}H-^{1}H TOCSY (Fig. 3D) clearly showed that this methine is in the same spin system as 26/27-CH3, indicating the hydroxylation occurred in the side chain. From HMBC (Fig. 3E), 26/27-CH3 (^{1}H at 0.91 ppm) showed strong correlation to this new methine (^{13}C at 78.4 ppm). In addition, 25-CH of this metabolite shifted to low field (^{1}H at 1.63 ppm and 13C at 34.6 ppm) compared with that of parent compound (^{1}H at 1.55 ppm and ^{13}C at 29.2 ppm) as a result of the deshielding effect from an adjacent hydroxyl group at 24 position. From the above analysis, the hydroxylation site can be unambiguously assigned to the 24-position.

3.3. Identification of Product C as 22-hydroxylumisterol3 (22(OH)L3) by NMR

The site of hydroxylation in the monohydroxy-L3, product C, was assigned to be at the 22-position based on the NMR spectra of this metabolite. First, none of the five methyl groups (18, 19, 21, 26, 27) are hydroxylated based on ^{1}H NMR and ^{1}H-^{13}C HSQC (Fig. 4A and B). ^{1}H-^{13}C HSQC revealed the presence of a new methine group at 3.58 ppm (^{13}C at 74.5 ppm, Fig. 4C). ^{1}H-^{1}H TOCSY (Fig. 4D) clearly showed that this methine is in the same spin system as 26/27-CH3, indicating the hydroxylation occurred in the side chain. From HMBC (Fig. 4E), 26/27-CH3 or 21-CH3 (^{1}H at 0.93 ppm) showed strong correlation to this new methine (^{13}C at 74.5 ppm). However, 25-CH (^{1}H at 1.57 ppm and ^{13}C at 29.5) was intact compared with the parent compound, L3. In addition, 20-CH of this metabolite shifted to low field (^{1}H at 1.66 ppm and ^{13}C at 44.3 ppm) compared with that of the parent compound (^{1}H at 1.38 ppm and ^{13}C at 38.1 ppm) most probably due to the deshielding effect from an

adjacent electron withdrawing group at C22. From the above analysis, the hydroxylation site can be unambiguously assigned to the 22-position.

3.4. Identification of Product A as 20,22-dihydroxylumisterol3 (20,22(OH)$_2$L3) by NMR

The site of hydroxylations in the dihydroxy-L3, product A, was unambiguously assigned to be at positions 20 and 22 based on the NMR spectra of this metabolite. We first identified the hydroxylation site at the 20-position; the doublet of 21-CH3 in L3 became a singlet in the metabolite (^{1}H at 1.18 ppm) (Fig. 5A, B), indicating the loss of scalar coupling from 20-CH. The 21-CH3 of this metabolite shifted to low field (^{1}H at 1.18 ppm) compared with that of the parent compound (^{1}H at 0.94 ppm) (Fig. 5A, B), indicating the deshielding effect by an adjacent electron withdrawing group. All five methyl groups (18, 19, 21, 26, and 27) were intact (Fig. 5A, B). From ^{1}H-^{13}C HMBC (Fig. 5C), 21-CH3 (^{1}H at 1.18 ppm) showed correlation to C-20 (^{13}C at 77.6 ppm) in addition to the expected correlation to C-17 (^{13}C at 57.2 ppm). By taking all these changes together, the presence of a 20-OH group in the metabolite is established. The assignment of the second hydroxylation at the 22-position is mainly based on ^{1}H-^{13}C HSQC and ^{1}H-^{13}C HMBC. ^{1}H-^{13}C HSQC revealed the presence of a new methine group at 3.29 ppm (^{13}C at 77.6 ppm, Fig. 5D). ^{1}H-^{1}H TOCSY (Fig. 5E) clearly showed that this methine is in the same spin system as 26/27-CH3, indicating this methine is in the same spin system as 26/27-CH3 (^{1}H at 0.92 ppm). From ^{1}H-^{13}C HMBC (Fig. 5C), 21-CH3 (^{1}H at 1.18 ppm) showed correlation to this new methine (^{13}C at 77.6 ppm). The coincident overlaps of 20-C (^{13}C at 77.6 ppm) and 22-C (^{13}C at 77.6 ppm) was consistent with that of 20,22(OH)$_2$D3 in which the C20 and C22 had identical ^{13}C chemical shifts (Tuckey et al., 2011). Thus, the second hydroxylation site was unambiguously assigned to be at the 22 position. Taken together the above analyses reveals that this metabolite is 20,22(OH)$_2$L3. The full assignments for this metabolite are summarized in Table 2 and expanded NMR spectra are shown in Supplemental Materials.

3.5. Further metabolism of 22(OH)L3, 24(OH)L3, 20,22(OH)$_2$L3 and product G by bovine CYP11A1

Incubation of 24(OH)L3 (product B) with CYP11A1 resulted in the formation of a single major product, identified from its retention time as dihydroxy-L3, product E (Fig. 6A). No further metabolism of product E to more polar products was detected. Product G (monohydroxy-L3) was converted to product F (Fig. 6B) which was collected and analyzed by mass spectrometry. It displayed the major ion at m/z = 439.2 $[M+Na]^+$, corresponding to M = 416.2, and was therefore identified as a dihydroxy-L3.

Incubation of 22(OH)L3 with CYP11A1 resulted in the expected production of 20,22(OH)$_2$L3 (product A), plus a small peak corresponding in retention time to pL (Fig. 6C). Another minor product with RT = 27 min (product H) was also observed as well as a product with RT = 29.4 min (product I). Consistent with this, incubation of 20,22(OH)$_2$L3 with CYP11A1 produced products H, I and pL (Fig. 6D). The peak for pL had an identical retention time to authentic standard, confirmed by spiking of the products with pL (Fig. 6E). It was further confirmed to be pL by mass spectrometry with major ions at m/z = 337.0 $[M+Na]^+$ and 315.1 $[M+H]^+$, corresponding to M = 314, as also seen for authentic standard. Minor products H and I produced from 20,22(OH)$_2$L3 were also collected and analyzed by

mass spectrometry. Both displayed the major ion at m/z = 455.1 $[M+Na]^+$, corresponding to M = 432.1, and were identified as trihydroxylumisterols. It is thus apparent that $20,22(OH)_2$L3 can undergo side chain cleavage, in a similar fashion to 20,22-dihydroxycholesterol and 20,22-dihydroxy-7-DHC (Slominski et al., 2012b; Tuckey, 2005) to produce pL. $20,22(OH)_2$L3 also undergoes further hydroxylation by CYP11A1 to two trihydroxylumisterols with the positions of the new hydroxyl groups not identified (see Discussion for a summary of pathways).

3.6. Kinetics of L3 metabolism by bovine CYP11A1

The initial rate of L3 metabolism by bovine CYP11A1 was measured at a range of L3 concentrations and data fitted to the Michaelis-Menten equation (not shown). This gave a K_m value of 39 ± 20 μM, a k_{cat} of 4.8 ± 1.3 min^{-1} (data are mean ± S.E. of the curve fit) and a catalytic efficiency of (k_{cat}/K_m) of 123 $mM^{-1}min^{-1}$. Kinetic parameters reported for vitamin D3 metabolism by CYP11A1 under identical conditions are K_m = 29.6 μM, k_{cat} = 19.7 min^{-1} and k_{cat}/K_m = 666 $mM^{-1}min^{-1}$, and for cholesterol metabolism are K_m = 9.1 μM, k_{cat} = 6.1 min^{-1} and k_{cat}/K_m = 670 $mM^{-1}min^{-1}$ (Tuckey et al., 2008b). Thus when dissolved in cyclodextrin, L3 is metabolized by CYP11A1 at approximately 20% of the catalytic efficiency reported for vitamin D3 and cholesterol.

3.7. Metabolism of L3 by human CYP11A1

To further illustrate the potential importance of the metabolism of L3 by CYP11A1, the ability of the human enzyme to metabolize L3 was tested. As for the bovine enzyme, the major products were 22(OH)L3, 24(OH)L3, $20,22(OH)_2$L3 and dihydroxy-L3 product E (Fig. 7). Identification was based on identical HPLC retention times to the products of the bovine enzyme using both a methanol–water gradient (Fig. 7) and an acetonitrile-water gradient (not shown). A greater proportion of $20,22(OH)_2$L3 to $20,24(OH)_2$L3 was seen for the human enzyme compared to the bovine enzyme suggesting that initial hydroxylation at C22 is favored by the human CYP11A1. Only a small peak corresponding to product G was detected for the human enzyme.

3.8. Metabolism of L3 by pig adrenal glands

To define the *in vivo* capability of tissues expressing CYP11A1 to metabolize L3, we incubated pig adrenals fragments *ex-vivo* with this sterol at concentrations of 50 μM and 500 μM for 20 h. Extracts of samples were analyzed by UPC LC-QTOF MS with EIC using m/z = 401.3 $[M+H]^+$; 383.3 $[M-H_2O+H]^+$, 365.3 $[M-2H_2O+H]^+$ or 423.3 $[M+Na]^+$ for monohydroxy-L3. This initial analysis revealed the presence of 3 peaks with retention times corresponding to standard 22(OH)L3, 24(OH)L3 and product G that were absent in negative controls incubated without substrate, with relative concentrations being highest when 500 μM was used as the substrate (not shown). To confirm the identification of products a preliminary separation and purification of metabolites by HPLC using an acetonitrile in water gradient was carried out (see Materials and Methods). Peaks corresponding to standards were collected and then analyzed using UPC LC-QTOF MS (Fig. 8). 22(OH)L3 (m/z = 383.3 $[M-H_2O+H]^+$), 24(OH)L3 (m/z = 423.3 $[M+Na]^+$) and monoxydroxy-L3 product G (m/z = 383.3 $[M-H_2O+H]^+$) were clearly identified in incubations of adrenal

fragments with 500 μM L3. These products were below the background noise in control samples incubated with vehicle only (Fig 8, D–F). Similar analyses were performed for dihydroxy-L3 derivatives and pL in extracts of adrenal fragments incubated with L3. While initial UPC LC-QTOF MS analysis for masses corresponding to 417.3 $[M+H]^+$; 399.3 $[M-H_2O+H]^+$, 381.3 $[M-2H_2O+H]^+$ or 439.3 $[M+Na]^+$ identified peaks with RTs corresponding to 20,22$(OH)_2$L3 and CYP11A1 product E, the pL signal was not clear above background. Therefore, these metabolites were purified by HPLC using an acetonitrile in water gradient as before, and then analyzed by UPC LC-QTOF MS. Fig. 9 clearly shows that all three products are made by adrenal fragments incubated with L3. The peaks with retention times corresponding to these metabolites were smaller (20,22$(OH)_2$L3 and pL) or undetectable in adrenals incubated with vehicle only.

4. Discussion

We have shown for the first time that L3 can be metabolized by CYP11A1 and identified C20, C22 and C24 as sites of hydroxylation of the L3 side chain. C22 and C24 are almost equally favored as the initial site of hydroxylation by the bovine enzyme, but C22 is preferred by the human enzyme. We did not detect production of 20(OH)L3 by CYP11A1 indicating that initial hydroxylation at C20 was not favored and only occurred after C22-hydroxylation, as reported for hydroxylation of cholesterol and 7-DHC by CYP11A1 (Slominski et al., 2012b; Tuckey, 2005). The 20,22$(OH)_2$L3 undergoes cleavage between carbons 20 and 22 to produce pL. This cleavage reaction is analogous to that of the well characterized cleavage of 20,22$(OH)_2$-cholesterol to pregnenolone (Tuckey, 2005), and 20,22$(OH)_2$-7-DHC which is a stereoisomer of 20,22$(OH)_2$L3, to produce 7-dehydropregnenolone (Slominski et al., 2012b). C24 has previously been identified as a site of hydroxylation of vitamin D2 and ergosterol by CYP11A1, substrates for which no cleavage of the side chain occurs (Slominski et al., 2005b; Nguyen et al., 2009). The pathways of L3 metabolism by CYP11A1 are summarized in Fig 10. As well as pL, two minor trihydroxy-L3 metabolites are produced from 20,22$(OH)_2$L3, with positions V and W of hydroxylation being unknown (Fig. 10). The site of hydroxylation X in Product G (X(OH)D3), which is not C20, C22 or C24, remains to be established. The likely position is C23 since this is between the two major sites of hydroxylation at C22 and C24 so will be close to the heme iron, and this is a known site of hydroxylation of the vitamin D3 side chain (Tuckey et al., 2008a, 2011). It is clear that modifications to the ring system of the CYP11A1 substrate as illustrated by comparing, cholesterol, 7-DHC, vitamin D3 and L3, influences the positioning of the side chain in the active site next to the heme group, determining the hydroxylation pattern and whether cleavage can occur. The structure of the ring system also influences the kinetics parameters for substrate metabolism, with 7-DHC and cholesterol being metabolized with a higher catalytic efficiency than vitamin D3 in a membrane reconstituted system (Slominski et al., 2004; Tuckey et al., 2008b). This study shows that L3 is metabolized with an efficiency that is approximately 20% of that for vitamin D3 and cholesterol when substrates are solubilized in a cyclodextrin solution.

To define whether CYP11A1 can metabolize L3 under *in vivo* conditions, we tested if adrenal gland fragments, which express a high level of CYP11A1, are capable of *ex-vivo* metabolism of exogenously added L3. We were able to detect the three major hydroproducts

of L3 metabolism with RT and masses corresponding to 22(OH)L3, 24(OH)L3 and 20,22(OH)$_2$L3. In addition, we detected a small amount of pL and a monohydroxy-L3 tentatively identified as product G made by the purified enzyme. These data indicate that tissues expressing CYP11A1 are capable of metabolizing L3 in a similar manner to the purified enzyme. Therefore, we propose that L3 after reaching the systemic circulation either from photo-production in the skin or oral delivery, can be metabolized by organs expressing high levels of CYP11A1, to novel L3 derivatives. It might also be directly metabolized in the skin which expresses some CYP11A1, although at significantly lower levels than in the adrenal cortex (Slominski et al., 1996, 2004, 2014a ; Thiboutot et al., 2003).

It has been postulated that unlike vitamin D3, neither L3 nor T3 affects calcium metabolism (Holick et al., 1981;Wacker and Holick, 2013). However, the synthetic hydroxyderivative of L3, 1,25-dihydroxy-L3, demonstrates biological activity apparently acting through binding to a second site on the vitamin D receptor (VDR) that mediates nongenomic responses (Dixon et al., 2011; Mizwicki et al., 2004; Rebsamen et al., 2002). Using chemical photosynthesis to generate vitamin D analogs with a short side chain (pD and aD compounds) we also generated pL and hydroxy-pL-derivatives (Zmijewski et al., 2008, 2009, 2011). Initial testing of their biological activity showed that pL inhibited the proliferation and stimulated the differentiation of leukemia cells (Slominski et al., 2010). Its 21- hydroxyderivative, 3β,21-dihydroxy-9β,10α-pregna-5,7-dien-20-one (21(OH)pL3), also inhibited the proliferation of keratinocytes and melanoma cells, with high potency in the case of melanotic SKMEL-188 melanoma cells (Zmijewski et al., 2011). This steroid also stimulated translocation of a VDR-green-fluorescent-protein construct from the cytoplasm to the nucleus of melanoma cells suggesting that such effects can be mediated by the VDR. However, 17,20(OH)$_2$pL showed lower activity towards melanoma cells than corresponding pD compounds (Zmijewski et al., 2009). Thus depending on cell type and chemical structure, synthetic lumisterol derivatives can have biological functions comparable to hydroxy-derivatives of vitamin D. These data also suggest that polar metabolites of L3 produced by the action of CYP11A1, could have similar biological activities. This opens new opportunities for testing the hypothesis that metabolism of L3 by CYP11A1 can produce biologically active metabolites acting either locally or systemically with their mechanism of action to be determined, a subject of our future research.

In summary, we demonstrate for the first time that CYP11A1 either *in vitro* or *ex vivo* (adrenal gland fragments) can metabolize L3 to several metabolites including 22(OH)L3, 24(OH)L3, 20,22(OH)$_2$L3 and pL, emphasizing a broader role for this enzyme that is aside from its role in initiating steroid hormone synthesis.

Supplementary Material

Refer to Web version on PubMed Central for supplementary material.

Acknowledgments

This work was supported by The University of Western Australia (RCT), NIH grants 2R01AR052190-A6, 1R01AR056666-01A2(AS), and 1R21AR063242-01A1, 1S10OD010678-01, and 1S10RR026377-01 (WL). The

content is solely the responsibility of the authors and does not necessarily represent the official views of the National Institutes of Health.

Abbreviations

cyclodextrin	2-hydroxypropyl-β-cyclodextrin
7-DHC	7-dehydrocholesterol
L3	lumisterol3
20(OH)L3	20-hydroxylumisterol3
22(OH)L3	22-hydroxylumisterol3
24(OH)L3	24-hydroxylumisterol3
20,22(OH)$_2$L3	20,22-dihydroxylumisterol3
pL	pregnalumisterol
RT	retention time
T3	tachysterol3

References

Clarke MW, Tuckey RC, Gorman S, Holt B, Hart PH. Optimized 25-hydroxyvitamin D analysis using liquid-liquid extraction with 2D separation with LC/MS/MS detection, provides superior precision compared to conventional assays. Metabolomics. 2013; 9:1031–1040.

De Caprio J, Yun J, Javitt NB. Bile acid and sterol solubilization in 2-hydroxypropyl-β-cyclodextrin. J Lipid Res. 1992; 33:441–443. [PubMed: 1569391]

Dixon KM, Norman AW, Sequeira VB, Mohan R, Rybchyn MS, Reeve VE, Halliday GM, Mason RS. 1alpha,25(OH)-vitamin D and a nongenomic vitamin D analogue inhibit ultraviolet radiation-induced skin carcinogenesis. Cancer Prev Res. 2011; 4:1485–1494.

Guryev O, Carvalho RA, Usanov S, Gilep A, Estabrook RW. A pathway for the metabolism of vitamin D3: unique hydroxylated metabolites formed during catalysis with cytochrome P450scc (CYP11A1). Proc Natl Acad Sci USA. 2003; 100:14754–14759. [PubMed: 14657394]

Holick MF. Vitamin D: a millennium perspective. J Cell Biochem. 2003; 88:296–307. [PubMed: 12520530]

Holick MF, MacLaughlin JA, Clark MB, Holick SA, Potts JT Jr, Anderson RR, Blank IH, Parrish JA, Elias P. Photosynthesis of previtamin D3 in human skin and the physiologic consequences. Science. 1980; 210:203–205. [PubMed: 6251551]

Holick MF, MacLaughlin JA, Doppelt SH. Regulation of cutaneous previtamin D_3 photosynthesis in man: Skin pigment in not an essential regulator. Science. 1981; 211:590–593. [PubMed: 6256855]

MacLaughlin JA, Anderson RR, Holick MF. Spectral character of sunlight modulates photosynthesis of previtamin D_3 and its photoisomers in human skin. Science. 1982; 216:1001–1003. [PubMed: 6281884]

Mizwicki MT, Keidel D, Bula CM, Bishop JE, Zanello LP, Wurtz JM, Moras D, Norman AW. Identification of an alternative ligand-binding pocket in the nuclear vitamin D receptor and its functional importance in 1alpha,25(OH)2-vitamin D3 signaling. Proc Natl Acad Sci USA. 2004; 101:12876–12881. [PubMed: 15326291]

Nguyen MN, Slominski A, Li W, Ng YR, Tuckey RC. Metabolism of vitamin D2 to 17,20,24-trihydroxyvitamin D2 by cytochrome P450scc (CYP11A1). Drug Metab Dispos. 2009; 37:761–767. [PubMed: 19116262]

Norval M, Bjorn LO, de Gruijl FR. Is the action spectrum for the UV-induced production of previtamin D_3 in human skin correct? Photochem Photobiol. 2010; 9:11–17.

Rebsamen MC, Sun J, Norman AW, Liao JK. 1alpha,25-dihydroxyvitamin D3 induces vascular smooth muscle cell migration via activation of phosphatidylinositol 3-kinase. Circ Res. 2002; 91:17–24. [PubMed: 12114317]

Slominski A, Ermak G, Mihm M. ACTH receptor, CYP11A1, CYP17 and CYP21A2 genes are expressed in skin. J Clin Endocrinol Metab. 1996; 81:2746–2749. [PubMed: 8675607]

Slominski AT, Janjetovic Z, Fuller BE, Zmijewski MA, Tuckey RC, Nguyen MN, Sweatman T, Li W, Zjawiony J, Miller D, Chen TC, Lozanski G, Holick MF. Products of vitamin D3 or 7-dehydrocholesterol metabolism by cytochrome P450scc show anti-leukemia effects, having low or absent calcemic activity. PLoS ONE. 2010; 5(3):e9907. [PubMed: 20360850]

Slominski A, Janjetovic Z, Tuckey RC, Nguyen MN, Bhattacharya KG, Wang J, Li W, Jiao Y, Gu W, Brown M, Postlethwaite AE. 20S-Hydroxyvitamin D3, noncalcemic product of CYP11A1 action on vitamin D3, exhibits potent antifibrogenic activity in vivo. J Clin Endocr Metab. 2013; 98:E298–E303. [PubMed: 23295467]

Slominski AT, Kim TK, Chen J, Nguyen MN, Li W, Yates CR, Sweatman T, Janjetovic Z, Tuckey RC. Cytochrome P450scc-dependent metabolism of 7-dehydrocholesterol in placenta and epidermal keratinocytes. Int J Biochem Cell Biol. 2012b; 44:2003–2018. [PubMed: 22877869]

Slominski AT, Kim TK, Li W, Yi AK, Postlethwaite A, Tuckey RC. The role of CYP11A1 in the production of vitamin D metabolites and their role in the regulation of epidermal functions. J Steroid Biochem Mol Biol. 2014a

Slominski AT, Kim TK, Shehabi HZ, Semak I, Tang EKY, Nguyen MN, Benson HAE, Korik E, Janjetovic Z, Chen J, Yates CR, Postlethwaite A, Li W, Tuckey RC. *In vivo* evidence for a novel pathway of vitamin D_3 metabolism initiated by P450scc and modified by CYP27B1. FASEB J. 2012a; 26:3901–3915. [PubMed: 22683847]

Slominski AT, Kim TK, Shehabi HZ, Tang EKY, Benson HAE, Semak I, Lin Z, Yates CR, Wang J, Li W, Tuckey RC. In vivo production of novel vitamin D2 hydroxy-derivatives by human placentas, epidermal keratinocytes, Caco-2 colon cells and the adrenal gland. Mol Cell Endocr. 2014b; 383:181–192.

Slominski AT, Kim TK, Takeda Y, Janjetovic Z, Brozyna AA, Skobowiat C, Wang J, Postlethwaite A, Li W, Tuckey RC, Jetten AM. RORα and RORγ are expressed in human skin and serve as receptors for endogenously produced noncalcemic 20-hydroxy- and 20,23-dihydroxyvitamin D. FASEB J. 2014c; 28:2775–2789. [PubMed: 24668754]

Slominski A, Semak I, Wortsman J, Zjawiony J, Li W, Zbytek B, Tuckey RC. An alternate pathway of vitamin D2 metabolism: Cytochrome P450scc (CYP11A1) mediated conversion to 20-hydroxyvitamin D2 and 17,20-dihydroxyvitamin D2. FEBS J. 2006; 273:2891–2901. [PubMed: 16817851]

Slominski A, Semak I, Zjawiony J, Wortsman J, Gandy MN, Li J, Zbytek B, Li W, Tuckey RC. Enzymatic metabolism of ergosterol by cytochrome P450scc (CYP11A1) to biologically active 17α,24-dihydroxyergosterol. Chem Biol. 2005b; 12:931–939. [PubMed: 16125105]

Slominski A, Semak I, Zjawiony J, Wortsman J, Li W, Szczesniewski A, Tuckey RC. The cytochrome P450scc system opens an alternate pathway of vitamin D3 metabolism. FEBS J. 2005a; 272:4080–4090. [PubMed: 16098191]

Slominski A, Zjawiony J, Wortsman J, Semak I, Stewart J, Pisarchik A, Sweatman T, Marcos J, Dunbar C, Tuckey RC. A novel pathway for sequential transformation of 7-dehydrocholesterol and expression of the P450scc system in mammalian skin. Eur J Biochem. 2004; 271:4178–4188. [PubMed: 15511223]

Slominski A, Zmijewski MA, Semak I, Sweatman T, Janjetovic Z, Li W, Zjawiony JK, Tuckey RC. Sequential metabolism of 7-dehydrocholesterol to steroidal 5,7-dienes in adrenal glands and its biological implication in the skin. PLoS ONE. 2009; 4(2):e4309. [PubMed: 19190754]

Strushkevich N, MacKenzie F, Cherkesova T, Grabovec I, Usanov S, Park H. Structural basis for pregnenolone biosynthesis by the mitochondrial monooxygenase system. Proc Natl Acad Sci USA. 2011; 108:10139–10143. [PubMed: 21636783]

Thiboutot D, Jabara S, McAllister JM, Sivarajah A, Gilliland K, Cong Z, Clawson G. Human skin is a steroidogenic tissue: steroidogenic enzymes and cofactors are expressed in epidermis, normal sebocytes, and an immortalized sebocyte cell line (SEB-1). J Invest Dermatol. 2003; 120:905–914. [PubMed: 12787114]

Tuckey RC. Progesterone synthesis by the human placenta. Placenta. 2005; 26:273–281. [PubMed: 15823613]

Tuckey RC, Li W, Shehabi HZ, Janjetovic Z, Nguyen MN, Kim TK, Chen J, Howell DE, Benson HAE, Sweatman T, Baldisseri DM, Slominski A. Production of 22-hydroxy metabolites of vitamin D_3 by cytochrome P450scc (CYP11A1) and analysis of their biological activities on skin cells. Drug Metab Dispos. 2011; 39:1577–1588. [PubMed: 21677063]

Tuckey RC, Li W, Zjawiony JK, Zmijewski MA, Nguyen MN, Sweatman T, Miller D, Slominski A. Pathways and products for the metabolism of vitamin D3 by cytochrome P450scc (CYP11A1). FEBS J. 2008a; 275:2585–2596. [PubMed: 18410379]

Tuckey RC, Nguyen MN, Chen J, Slominski AT, Baldisseri DM, Tieu EW, Li W. Human cytochrome P450scc (CYP11A1) catalyses epoxide formation with ergosterol. Drug Metab Dispos. 2012; 40:436–444. [PubMed: 22106170]

Tuckey RC, Nguyen MN, Slominski A. Kinetics of vitamin D3 metabolism by cytochrome P450scc (CYP11A1) in phospholipid vesicles and cyclodextrin. Int J Biochem Cell Biol. 2008b; 40:2619–2626. [PubMed: 18573681]

Tuckey RC, Sadleir J. The concentration of adrenodoxin reductase limits cytochrome P450scc activity in the human placenta. Eur J Biochem. 1999; 263:319–325. [PubMed: 10406938]

Tuckey RC, Stevenson PM. Properties of bovine luteal cytochrome P-450scc incorporated into artificial phospholipid vesicles. Int J Biochem. 1984; 16:497–503. [PubMed: 6724104]

Wacker M, Holick MF. Sunlight and vitamin D. A global perspective for health. Dermatoendocrinol. 2013; 5:1–58. [PubMed: 24494037]

Wang J, Slominski A, Tuckey RC, Janjetovic Z, Kulkarni A, Chen J, Postlethwaite AE, Miller D, Li W. 20-Hydroxyvitamin D3 inhibits proliferation of cancer cells with high efficacy while being non-toxic. Anticancer Res. 2012; 32:739–746. [PubMed: 22399586]

Woods ST, Sadleir J, Downs T, Triantopoulos T, Headlam MJ, Tuckey RC. Expression of catalytically active human cytochrome P450scc in *Escherichia coli* and mutagenesis of isoleucine-462. Arch Biochem Biophys. 1998; 353:109–115. [PubMed: 9578606]

Zmijewski MA, Li W, Chen J, Kim TK, Zjawiony JK, Sweatman TW, Miller DD, Slominski AT. Synthesis and photochemical transformation of 3beta,21-dihydroxypregna-5,7-dien-20-one to novel secosteroids that show anti-melanoma activity. Steroids. 2011; 76:193–203. [PubMed: 21070794]

Zmijewski MA, Li W, Zjawiony JK, Sweatman TW, Chen J, Miller DD, Slominski AT. Synthesis and photo-conversion of androsta- and pregna-5,7-dienes to vitamin D3-like derivatives. Photochem Photobiol Sci. 2008; 7:1570–1576. [PubMed: 19037511]

Zmijewski MA, Li W, Zjawiony JK, Sweatman TW, Chen J, Miller DD, Slominski AT. Photo-conversion of two epimers (20R and 20S) of pregna-5,7-diene-3beta, 17alpha, 20-triol and their bioactivity in melanoma cells. Steroids. 2009; 74:218–228. [PubMed: 19028513]

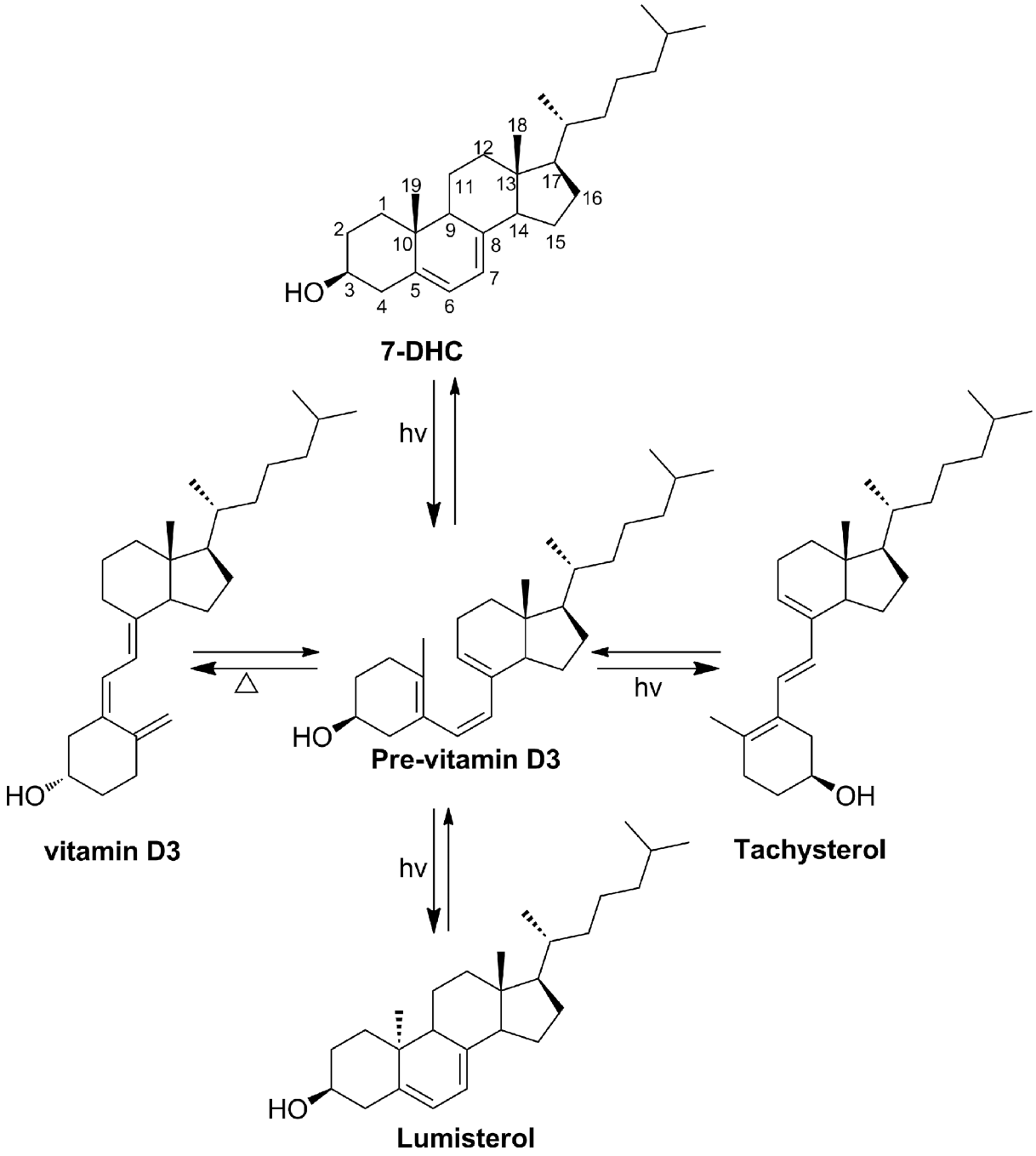

Fig. 1.
Photosynthesis of previtamin D3, tachysterol and lumisterol.

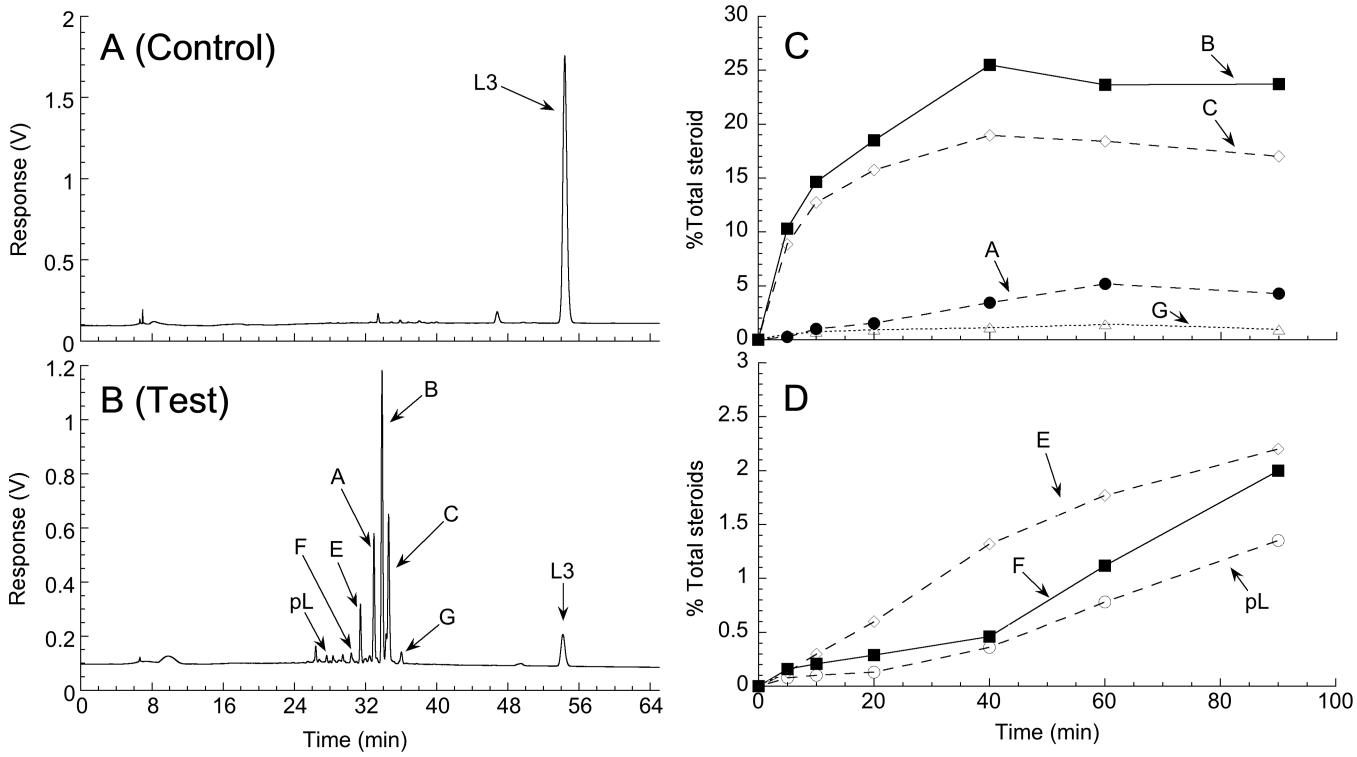

Fig. 2.

Analysis of the products of L3 metabolism by CYP11A1. (A,B) HPLC analysis of L3 metabolites. L3 (20 μM) in 0.45% cyclodextrin was incubated with 1.0 μM CYP11A1 for 3 h at 37°C in a reconstituted system containing adrenodoxin reductase (0.4 μM), adrenodoxin (15 μM) and NADPH (50 μM). Products were extracted with dichloromethane and analyzed by HPLC using a methanol-water gradient (see Experimental Procedures). A, Zero-time control incubation; B, Test incubation. (C,D) Time courses for the metabolism of L3 by CYP11A1. L3 (50 μM) in 0.45% cyclodextrin was incubated with 1.0 μM CYP11A1 and products analyzed by HPLC. (C) major initial products; (D) minor products.

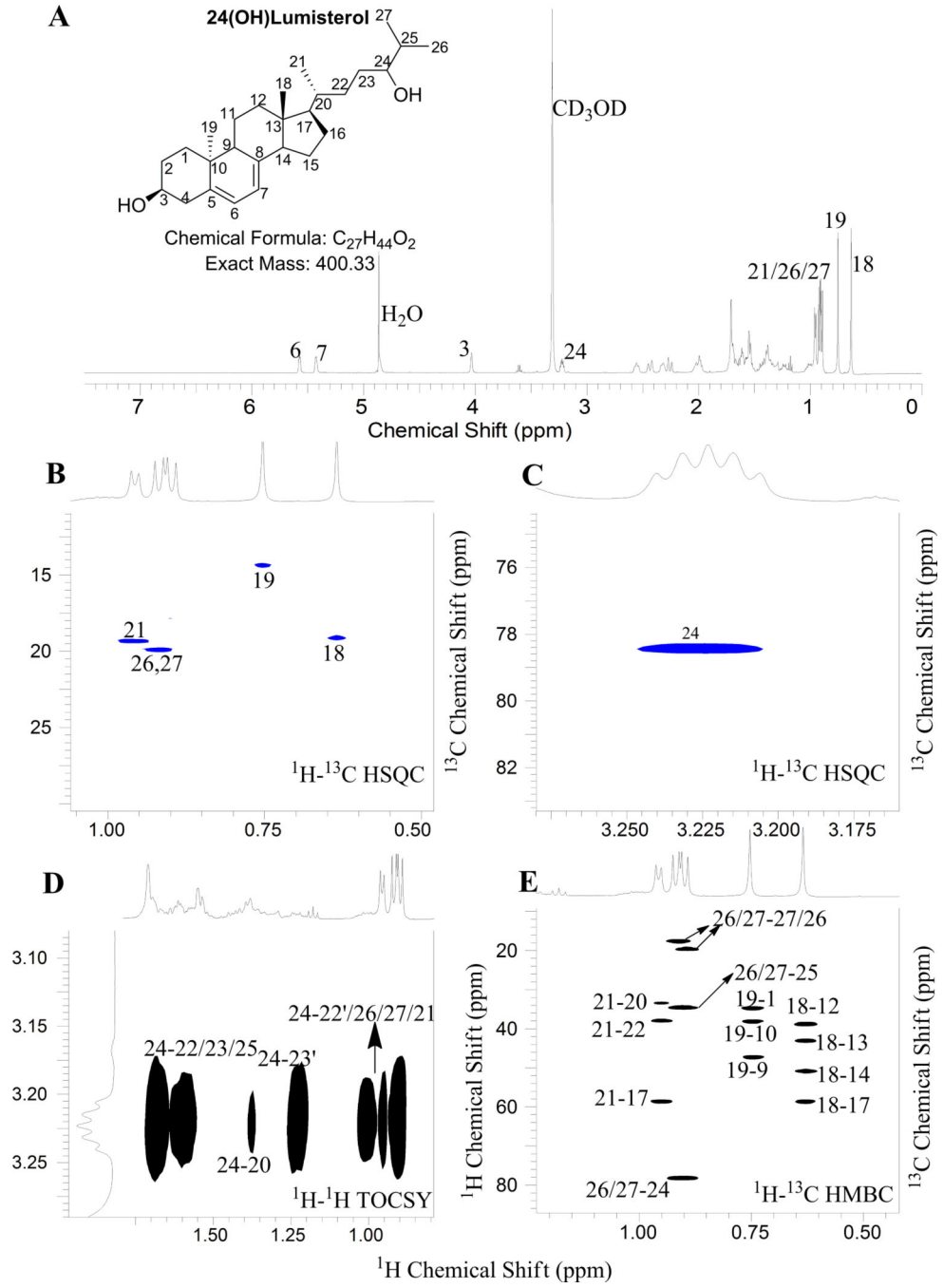

Fig. 3.

NMR analysis of Product B (24(OH)L3)

(A) 1D Proton; (B),(C) ^{1}H–^{13}C HSQC; (D) ^{1}H–^{1}H TOCSY; (E) ^{1}H–^{13}C HMBC

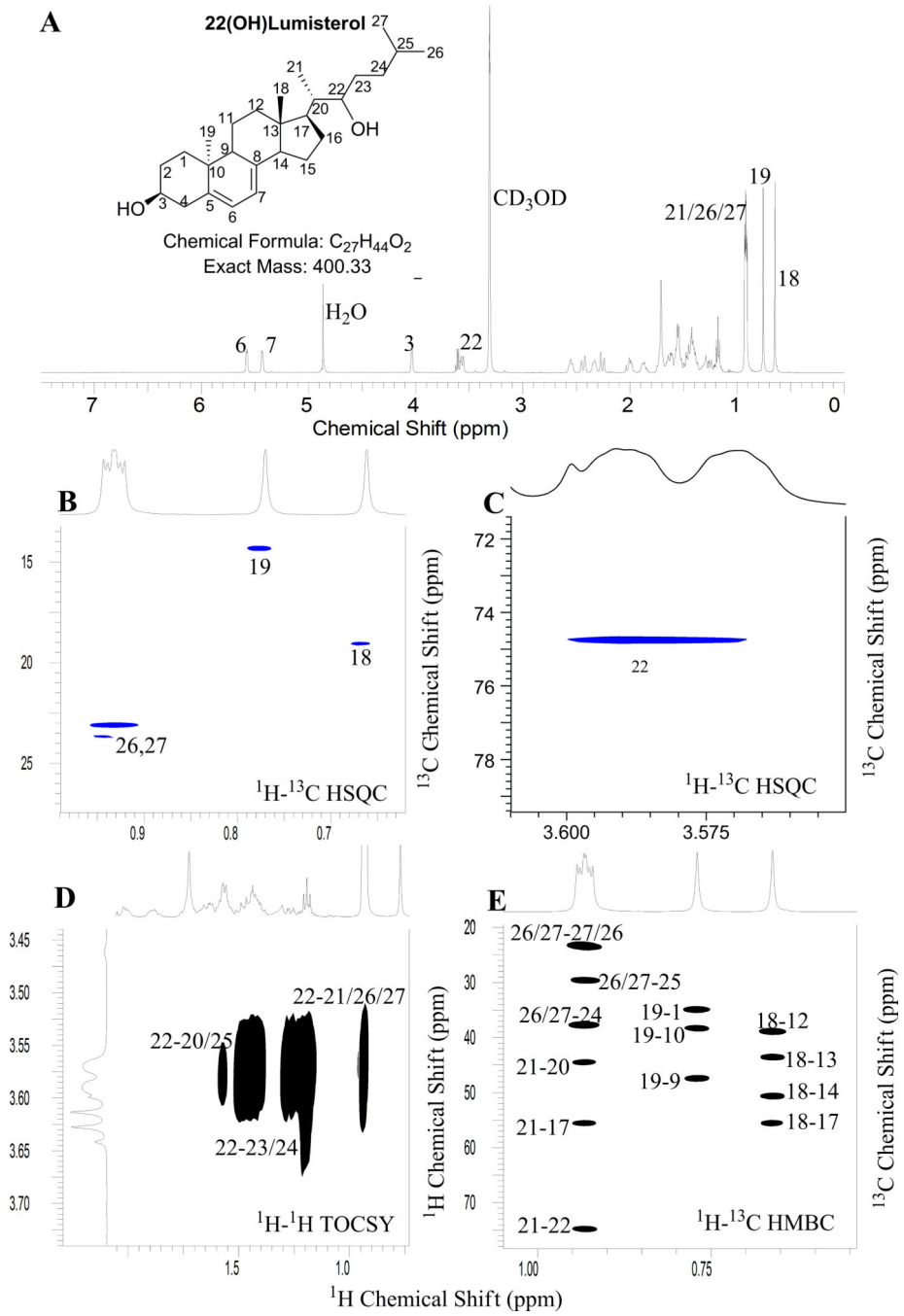

Fig. 4.

NMR analysis of product C (22(OH)L3)

(A) 1D Proton; (B),(C) ^{1}H–^{13}C HSQC; (D) ^{1}H–^{1}H TOCSY; (E) ^{1}H–^{13}C HMBC.

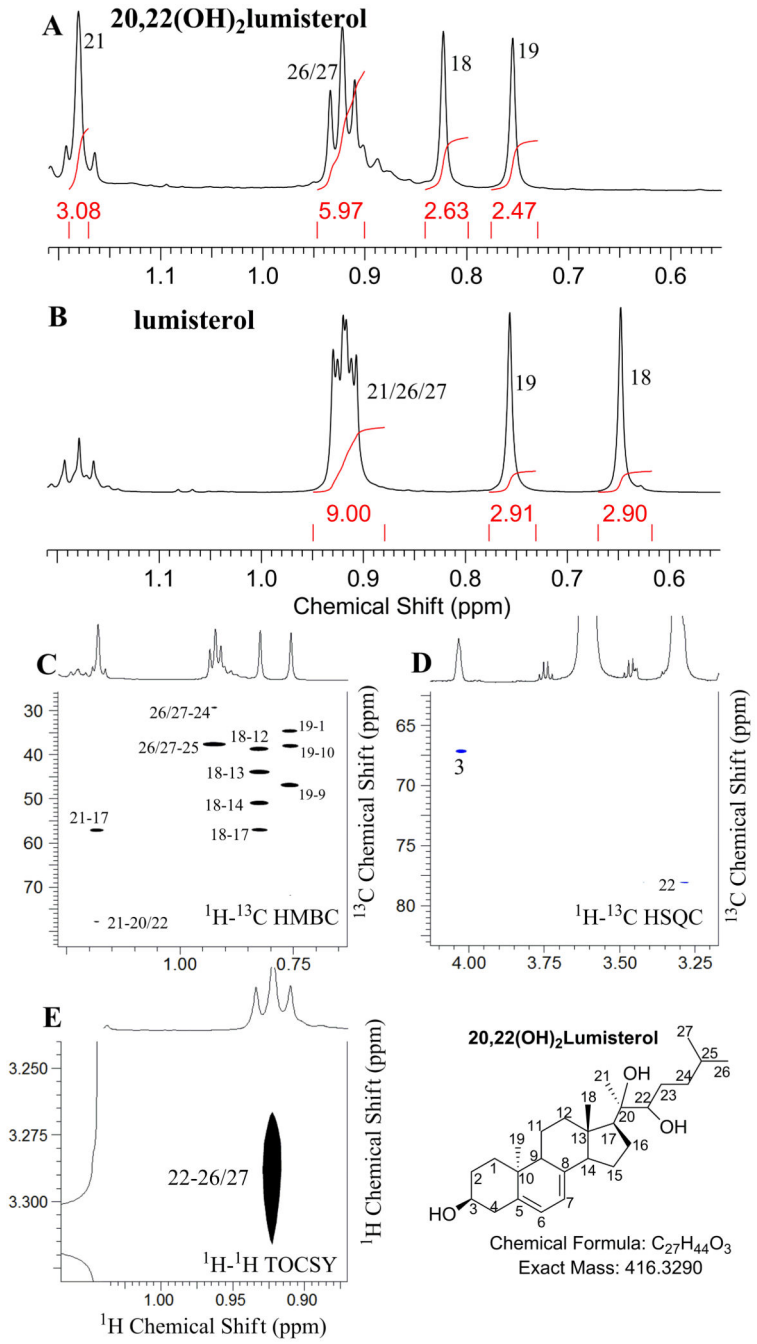

Fig. 5.

NMR analysis of product A (20,22(OH)$_2$L3)

(A) 1D Proton of 20,22(OH)$_2$L3; (B) 1D Proton of lumisterol; (C) ^{1}H–^{13}C HMBC; (D) ^{1}H–^{13}C HSQC; (E) ^{1}H–^{1}H TOCSY

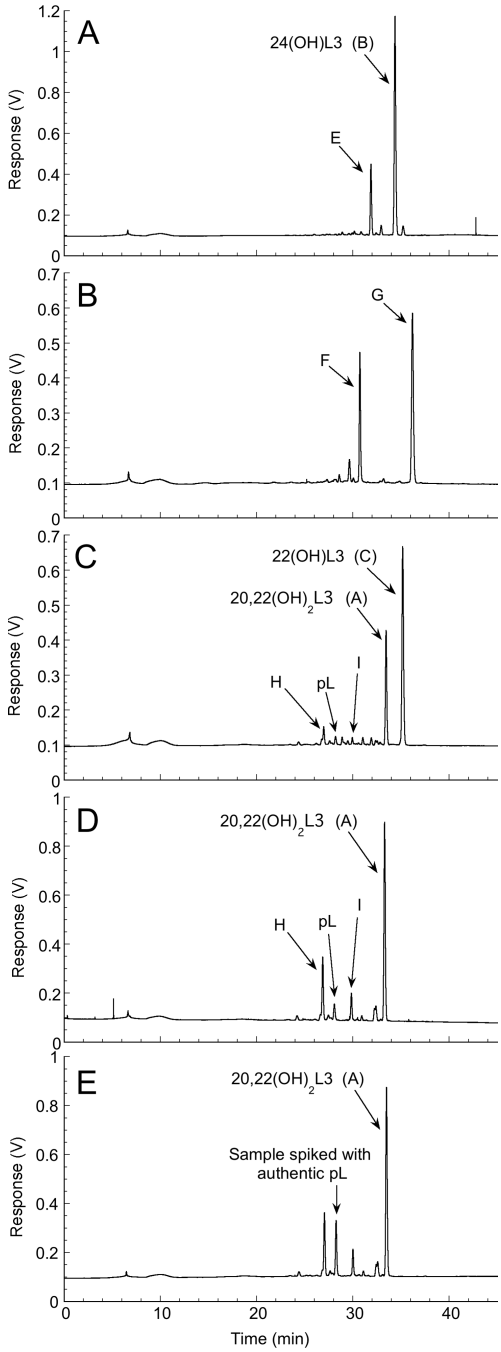

Fig. 6.

Further metabolism of L3 products by CYP11A1. 22(OH)L3, 24(OH)L3, 20,22(OH)$_2$L3 or Product G (20 μM in 0.45% cyclodextrin) were incubated with 2 μM CYP11A1 for 1 h, as in Fig. 2. Products were extracted with dichloromethane and analyzed by HPLC using a methanol-water gradient. Chromatograms show metabolites produced from (A) 24(OH)L3, product B; (B) monohydroxylumisterol, product G; (C) 22(OH)L3, product C; (D) 20,22(OH)$_2$L3, product A. (E) reaction mixture from 20,22(OH)$_2$L3 spiked with authentic pL.

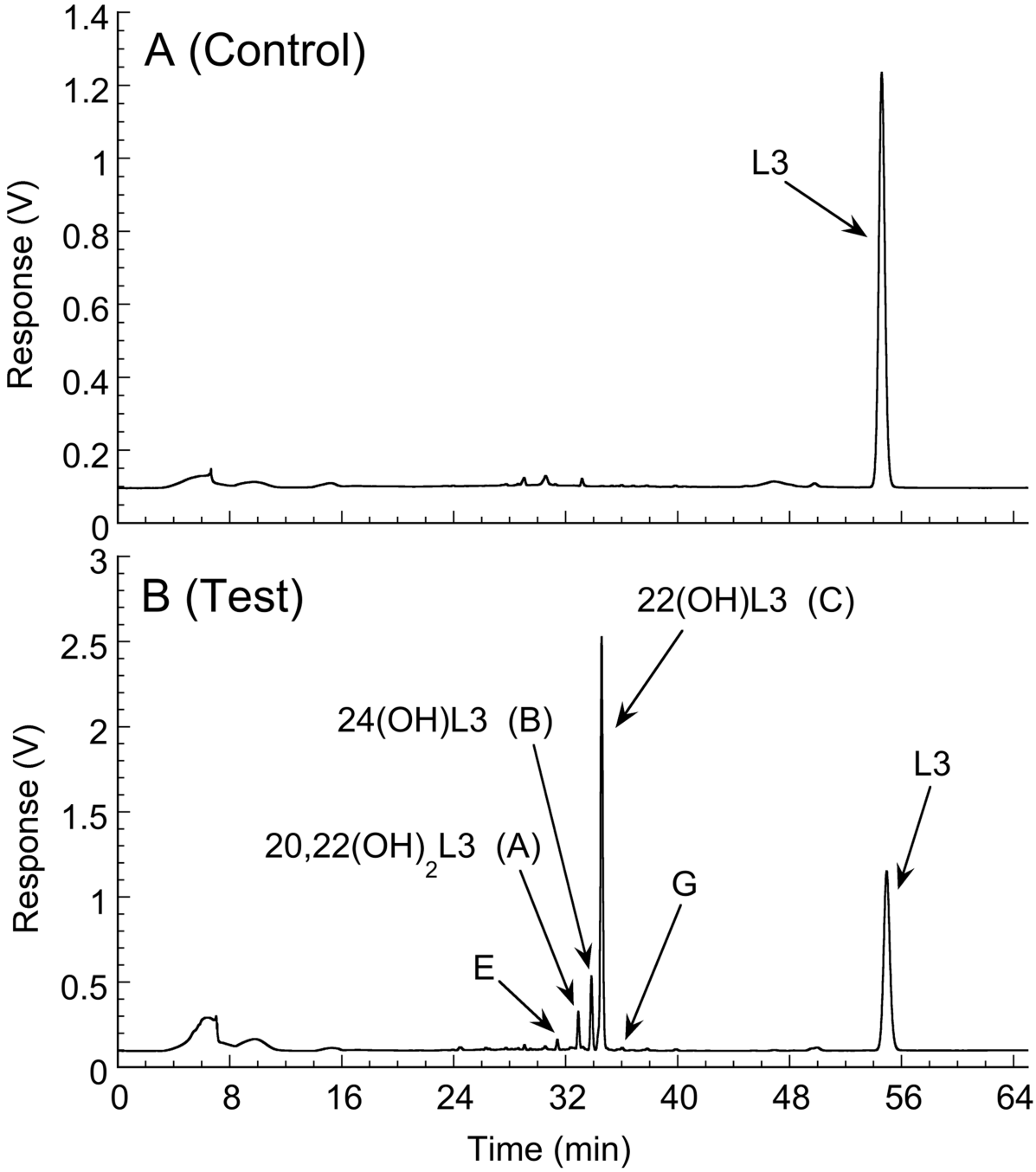

Fig. 7.

Metabolism of L3 by human CYP11A1. L3 (25 μM) in 0.45% cyclodextrin was incubated with 2.0 μM human CYP11A1 for 3 h at 37°C as for Fig. 2. Products were extracted with dichloromethane and analyzed by HPLC using a methanol-water gradient. (A) Control incubation with NADPH omitted; (B) Test incubation.

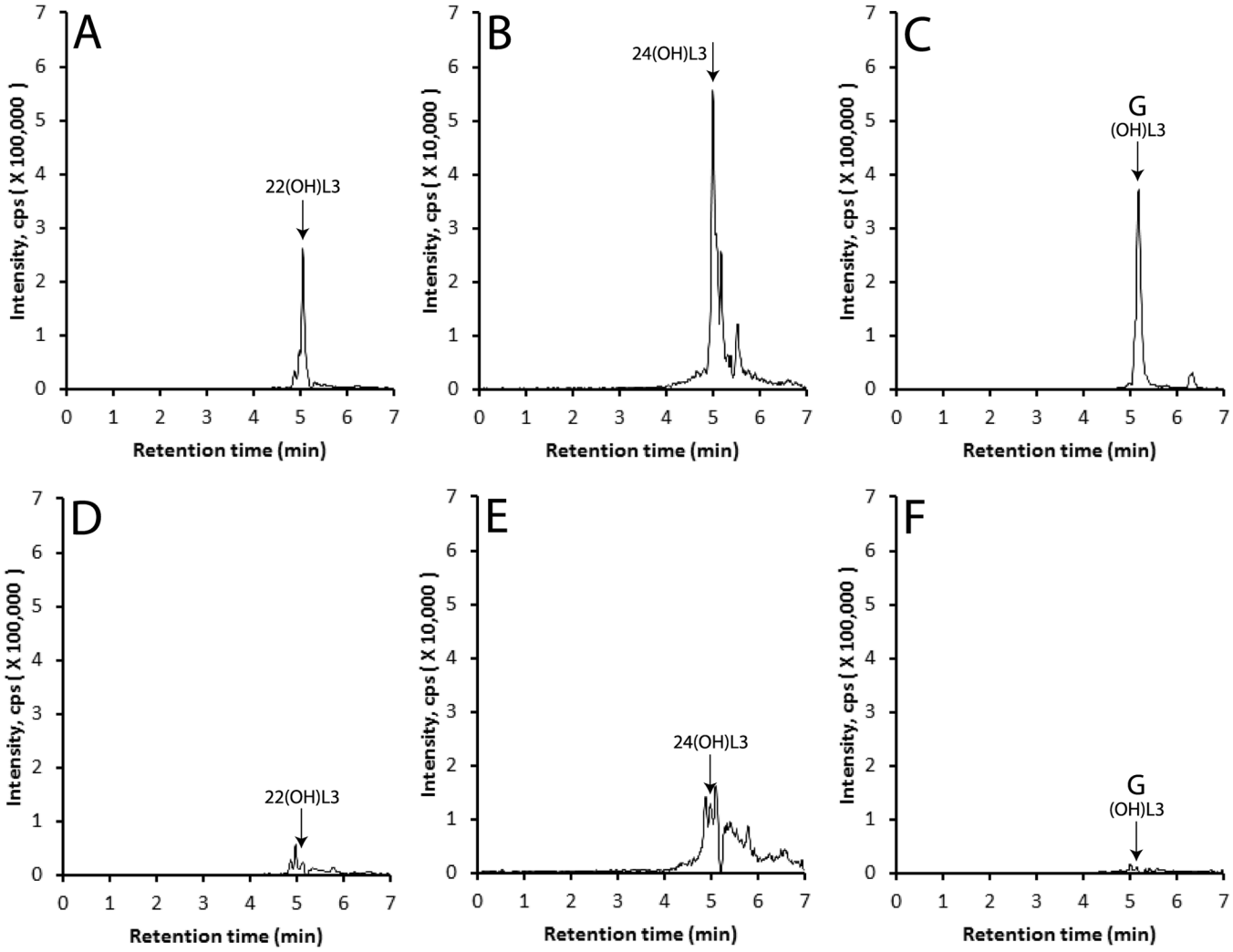

Fig. 8.

Production of monohydroxy-L3 in by pig adrenal fragments. L3 was incubated with pig adrenal fragments for 20 h, the metabolites extracted and a preliminary separation carried out by HPLC using an acetonitrile in water gradient. The collected metabolites were then analyzed by LC-MS qTOF) as described in the Materials and Methods. The EIC (extracted ion chromatogram) was analyzed using m/z = 383.3 $[M\text{-}H_2O+H]^+$ for 20(OH)L3 and 24(OH)L3, and m/z = 423.3 $[M+Na]^+$ for 24(OH)L3. (A), (B) and (C) pig adrenals incubated with 500 μM L3; (D), (E) and (F) pig adrenals incubated with vehicle only. (A) and (D) 22(OH)L3; (B) and (E) 24(OH)L3; (C) and (F), CYP11A1 metabolite (OH)L3, product G.

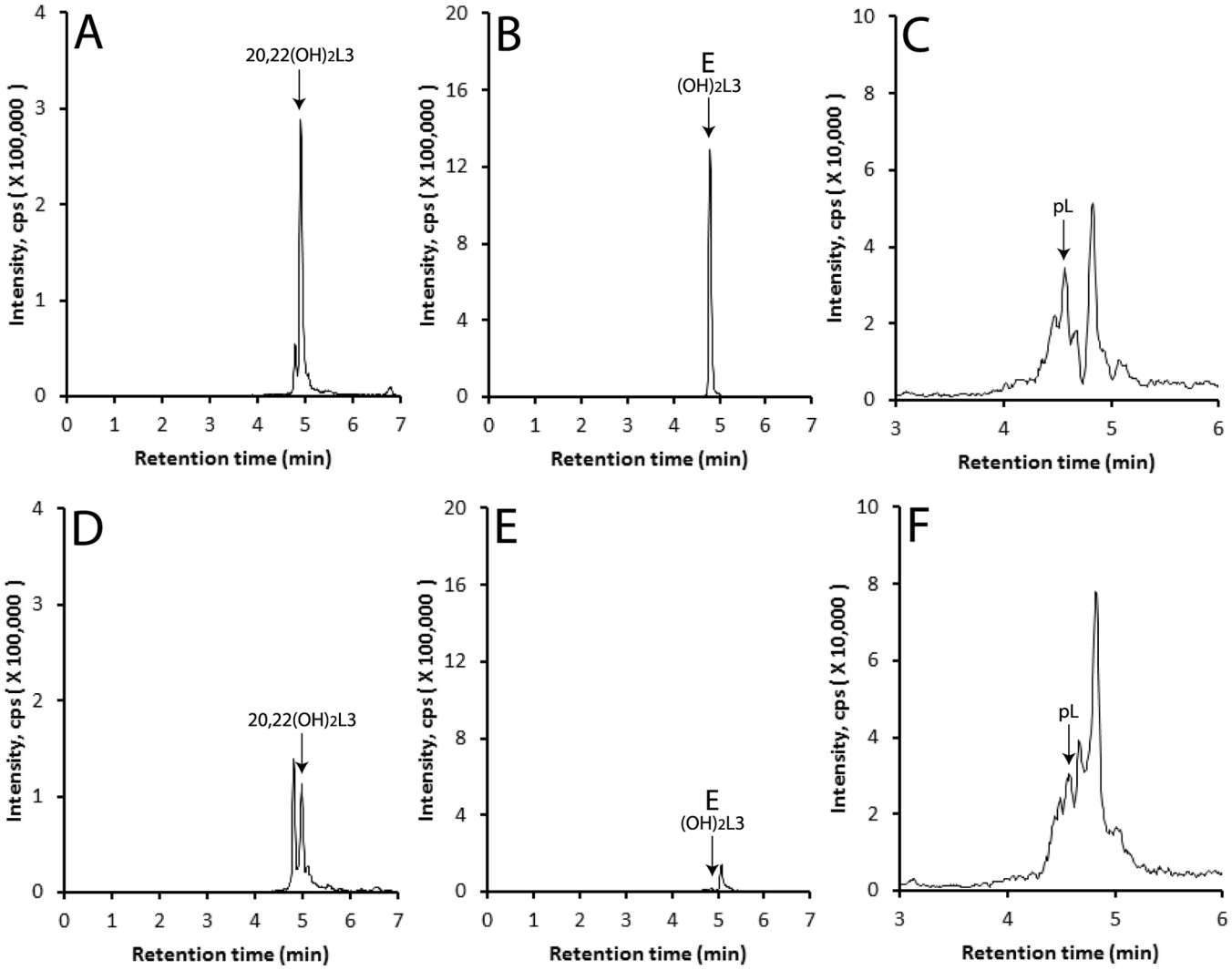

Fig. 9.

Production of dihydroxy-L3 and pL by pig adrenal fragments. L3 was incubated with adrenal fragments for 20 h, the metabolites extracted and a preliminary separation done by HPLC as in Fig. 10. Metabolites were then analyzed by LC-MS (qTOF) as described in the Materials and Methods. The EIC (extracted ion chromatogram) was analyzed using m/z = 439.3 $[M+Na]^+$ for 20,22$(OH)_2$L3 and unknown dihydroxy-L3, and 297.2 $[M-H_2O+H]^+$ for pL3. (A), (B) and (C) pig adrenals incubated with 500 μM L3; (D), (E) and (F) pig adrenals incubated with vehicle only. (A) and (D) 20,22$(OH)_2$L3; (B) and (E) CYP11A1 metabolite $(OH)_2$L3, product E; (C) and (F), pL.

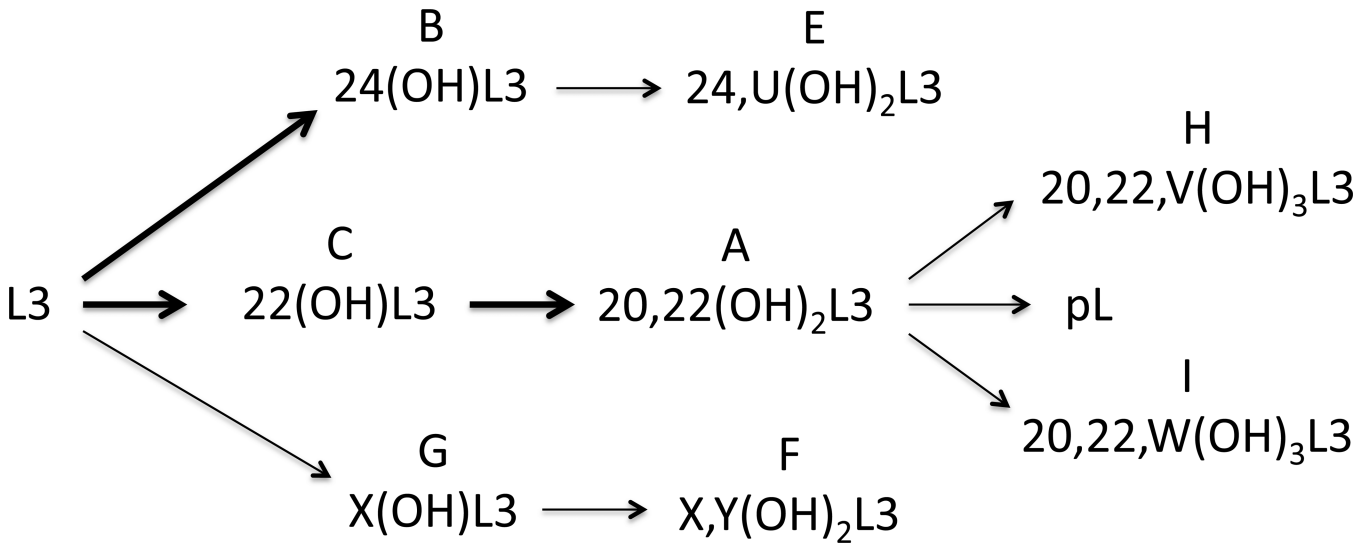

Fig. 10.

Summary of the pathways for metabolism of L3 by CYP11A1. The major pathways with products being identified by NMR are shown with bold arrows. Minor pathways are shown with thin arrows. U, V, W, X and Y are positions where the site of hydroxylation is unknown. Letters above metabolite names refer to the original product labels as defined in Fig. 2 and Fig. 6.

Table 1

High resolution mass spectrometry analyses of the major L3 metabolites. The error between the theoretical and observed mass to charge (m/z) ratio is less than 1 ppm (parts per million), well within the generally accepted limit of 5 ppm in high resolution mass spectrometry measurements. See sections 3.2–3.4 for the NMR identification (shown in parenthesis) of products C, B and A.

Metabolite	Observed m/z value	Theoretical m/z value	Predicted elemental composition	m/z error (ppm)
C (22(OH)L3)	423.3235	423.3239	$C_{27}H_{44}O_2Na$	−0.9
B (24(OH)L3)	423.3242	423.3239	$C_{27}H_{44}O_2Na$	0.7
G	423.3237	423.3239	$C_{27}H_{44}O_2Na$	−0.5
A (20,22$(OH)_2$L3)	439.3185	439.3188	$C_{27}H_{44}O_3Na$	−0.7
E	439.3190	439.3188	$C_{27}H_{44}O_3Na$	0.5

Int J Biochem Cell Biol. Author manuscript; available in PMC 2015 October 01.

Table 2

NMR chemical shift assignments for 22(OH)L3, 24(OH)L3 and 20,22(OH)$_2$L3. The solvent for NMR was CD_3OD.

	22(OH)L3 (Product C)		20,22(OH)$_2$L3 (Product A)		24(OH)L3 (Product B)		L3 (Parent)	
Atom	**^{1}H**	**^{13}C**	**^{1}H**	**^{13}C**	**^{1}H**	**^{13}C**	**^{1}H**	**^{13}C**
1	1.73,1.64	34.9	1.71,1.61	34.6	1.70,1.60	35.0	1.71,1.62	34.8
2	1.72	30.0	1.71	29.7	1.74	30.1	1.72	29.7
3	4.05	67.2	4.03	67.2	4.04	66.9	4.05	67.3
4	2.45, 2.27	39.1	2.43, 2.27	38.8	2.44, 2.27	39.2	2.43, 2.27	39.0
5	NA[a]	141.1	NA	141.0	NA	140.8	NA	141.0
6	5.59	122.0	5.58	122.1	5.58	122.0	5.58	122.0
7	5.45	117.1	5.44	117.1	5.43	117.0	5.43	116.9
8	NA	NI[b]	NA	NI	NA	NI	NA	NI
9	2.36	47.4	2.34	47.0	2.32	47.3	2.32	47.3
10	NA	38.3	NA	37.8	NA	38.0	NA	38.2
11	1.74, 1.47	23.8	NI	NA	1.71, 1.43	23.8	1.70, 1.43	23.7
12	2.03, 1.56	38.8	NI	38.9	2.00, 1.54	38.9	1.99, 1.55	38.7
13	NA	43.5	NI	44.0	NA	43.1	NA	43.0
14	2.57	50.6	2.56	51.1	2.56	50.9	2.56	51.0
15	1.58	20.2	1.57	20.3	1.55	20.4	1.55	20.0
16	1.89, 1.44	29.5	NI	NI	1.80, 1.46	34.8	2.01, 1.34	29.4
17	1.44	55.6	1.82	57.2	1.39	58.7	1.39	58.9
18	0.66	19.0	0.82	20.9	0.63	19.0	0.63	19.0
19	0.77	14.3	0.75	14.2	0.75	14.3	0.75	14.1
20	1.66	44.3	NA	77.6	1.38	38.0	1.38	37.7
21	0.93	23.6	1.18	20.7	0.96	19.3	0.94	19.2
22	3.58	74.5	3.29	77.6	1.70, 1.02	33.6	1.40, 1.05	37.3
23	1.43, 1.28	28.7	1.50, 1.22	NI	1.58, 1.24	32.1	1.42, 1.22	25.1
24	1.47, 1.20	37.5	1.47	38.0	3.22	78.4	1.19	40.9

Atom	22(OH)L3 (Product C)		20,22(OH)$_2$L3 (Product A)		24(OH)L3 (Product B)		L3 (Parent)	
	^{1}H	^{13}C	^{1}H	^{13}C	^{1}H	^{13}C	^{1}H	^{13}C
25	1.57	29.5	1.51	29.1	1.63	34.6	1.55	29.2
26	0.93	23.1	0.92	23.0	0.91	19.9	0.89	23.2
27	0.93	23.1	0.92	23.0	0.91	19.9	0.89	23.2

[a]NA – Not applicable (ternary carbons);

[b]NI – Not Identifiable (due to low resolution).